Massive Star Birth: A Crossroads of Astrophysics
Proceedings IAU Symposium No. 227, 2005
R. Cesaroni, M. Felli, E. Churchwell & C. M. Walmsley, eds.

doi:10.1017/S1743921305004746

The HST survey of the Orion Nebula region

Massimo Robberto†

Space Telescope Science Institute, 3700 San Martin Dr., Baltimore MD, 21212
email: robberto@stsci.edu

Abstract. The HST Treasury Program on the Orion Nebula Cluster has been recently completed (May 2005). Using 104 orbits of HST time we have imaged a field ∼1/6 of a square degree nearly centered on the Trapezium stars. The survey, made with ACS, WFPC2 and NICMOS-Camera 3 in parallel, has imaged this cornerstone region with unprecedented sensitivity (23-24 mag), dynamic range (∼12 mag), spatial resolution (50mas), and wide spectral coverage (9 filters from U to H). We have assembled the richest, most accurate and unbiased dataset of stellar photometry for pre-main-sequence objects ever obtained, an essential tool for understanding of the star formation process in regions dominated by massive OB stars.

Keywords. ISM: individual (M42, M43), stars: formation, stars: pre–main-sequence, ISM: jets and outflows, planetary systems: protoplanetary disks

1. Introduction

According to the current paradigm, dense, rich clusters dominated by massive OB stars represent the typical Galactic star-forming environment. The nearest of these region, the Orion Nebula (M42 = NGC1976) with its associated stellar cluster (ONC), therefore, plays a crucial role in our understanding of the star formation process.

For a variety of factors the Orion Nebula can be studied in great detail. It is relatively close ($d \sim 500$ pc), it lies away from the Galactic Plane ($b = -19°$), and in an anti-center quadrant ($l = 209°$) with minimal foreground confusion. The nebula is a blister HII region excavated on the surface of the OMC-1 Giant Molecular Cloud. The large total extinction of OMC-1 (up to $A_V = 50$–100 mag on its main ridge) strongly reduces background confusion. In front of the HII region there is only a foreground veil of neutral gas, marginally optically-thick. Its moderate extinction ($A_v \simeq 1.5$ mag) allows one to make detailed studies at visible wavelengths.

The rapid expansion of the HII region triggered by the most massive OB stars, θ^1Ori-C in particular, has exposed to our view the ONC, an extremely young ($t \sim 1$ Myr), rich ($n \sim 3500$ stars) and dense ($r \sim 2 \times 10^4$ stars pc^{-3} at the core) aggregate of pre-main-sequence (PMS) stars ranging from 45 $M_\odot$ to less than 0.02 $M_\odot$. The ONC provides the ideal laboratory where main questions on star formation can be addressed, such as the calibration of PMS evolutionary tracks, mass segregation and the variation of the initial mass function of single and multiple stars in different environments, the evolution of mass accretion rates vs. age and environment, disk dissipation in regions dominated by hard vs. soft-UV radiation, stellar multiplicity vs. disk fraction, etc.

Several groups have made deep IR surveys of the ONC core region using HST (Luhman *et al.* 2000), Keck (Hillenbrand & Carpenter 2000), UKIRT and Gemini (Lucas & Roche 2000, Lucas, Roche & Tamura 2005), NTT (Muench *et al.* 2002). These studies have probed the luminosity and mass function of the ONC down into the substellar mass

† Affiliated with the Space Telescopes Branch of the European Space Agency, ESTEC, Nordwijk, the Netherlands

Table 1. Filter selection

Camera	Filter	Exp. time (s)	repeat	notes
ACS/WFC	F435W (B)	420	1	
ACS/WFC	F555W (V)	385	1	
ACS/WFC	F775W (I)	385	1	
ACS/WFC	F850LP (z)	340	1	
ACS/WFC	F685N (Hα)	385	1	includes [NII]
WFPC2	F336W (U)	400	2	red-leak in I-band
WFPC2	F439W (B)	80	1	
WFPC2	F814W (I)	10	1	
WFPC2	F656N (Hα)	400	1	
NICMOS/3	F110W (J)	256	5	dithered
NICMOS/3	F160W (H)	192	4	dithered

regime, primarily on the basis of color-color and color-magnitude diagrams. However, IR photometry by itself provides no clear information on individual stars. Even the most basic relations, such as a K-band luminosity function, require statistical corrections, e.g. for the infrared excess of circumstellar disks.

The ONC can be better studied at optical wavelengths, due the low foreground extinction. Hillenbrand (1997) has assembled an extensive photometric and spectroscopic database, with V and I data down to $[I] \simeq 18$ mag. This survey, complete to 1.0 $M_\odot$ and with masses down to the H-burning limit, still provides the most complete existing database of stellar parameters (T_{eff}, L, age, mass) for a homogeneous sample of PMS stars. However, the available photometry is affected by the significant stellar variability of the ONC stars Herbst *et al.* 2002 and from a variety of observational factors, such as the bright nebular background, source crowding, binary companions, circumstellar disks and envelopes. The use of the Hubble Space Telescope is therefore essential, due to its unique combination of spatial resolution at visible wavelengths over a large fields of view.

An international team lead by the author proposed for the HST Cycle 13 a HST Treasury Program aimed at obtaining deep multi-color photometry of the entire ONC. The program, awarded with 104 HST orbits, has been recently completed (May 2005). It provides the richest, most accurate and unbiased dataset of stellar photometry for pre-main-sequence objects ever made. It is complemented by new ground-based observations aimed at extending the spectroscopic database both at visible and IR wavelengths, as well as at obtaining simultaneous broad-band photometry of the brightest cluster members, from the near-UV to the near-IR.

2. Observing Strategy

We have simultaneously used all imagers on board HST, i.e. ACS/WFC, WFPC2 and NICMOS/3, obtained in coordinated parallel mode. The Wide Field Channel of ACS has been used as a main instrument to obtain broad-band photometry in B, V, I and z-band analog filters. WFPC2 has been adopted to perform U-band (F336W) observations, as this filter is not available on ACS/WFC. With its short readout time, WFPC2 also packs much more efficiently the complementary short exposures needed to estimate the Balmer jump and the read-leak contamination to the F336W filter. NICMOS has been used in camera 3 mode, with the F110W and F160W filters, similar to the standard J and H passbands. In Table 1 we list the filters and the corresponding exposure times. All observations listed in Table 1 were performed within the $\simeq$40 min visibility windows of a single orbit.

https://doi.org/10.1017/S1743921305004746 Published online by Cambridge University Press

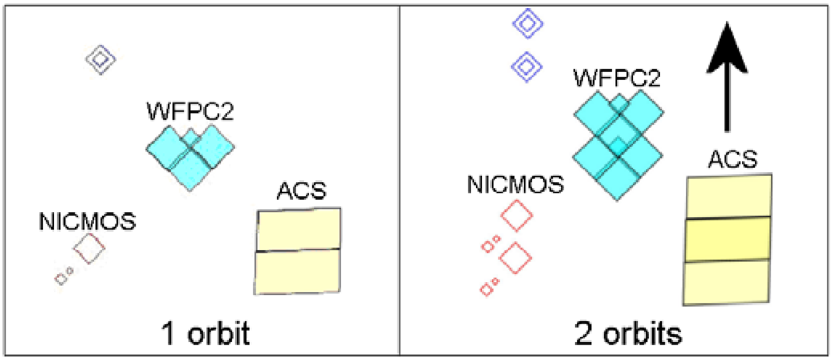

Figure 1. Left: location on the HST focal plane of the fields imaged by the three cameras. Right: fields overlay following a diagonal shift of WFPC2, or a transition from one CCD to the other of ACS.

The three instruments provide the following fields of view and scales:

- ACS/WFC: $202'' \times 202''$ field of view with $0.05''$/pixel scale,
- WFPC2: three adjacent Wide Field channels each $80'' \times 80''$ with $0.1''$/pixel scale, plus a high resolution channel (Planetary Camera) of $40'' \times 40''$ with $0.05''$/pixel scale, arranged in the characteristic chevron pattern;
- NICMOS Camera 3: $51.2'' \times 51.2''$ with $0.20''$pixel scale.

During each orbit the telescope pointing remained fixed. In order to image with NICMOS the largest possible field and allow for dithering and bad pixel removal, we used the Field Offset Mirror (FOM) internal to the NICMOS instrument as a scanning device. Since the FOM range was originally conservatively constrained, changes to the HST flight software were needed to implement a wider throw. During the 7 months duration of our program observations, the throw of the FOM has been progressively increased. Eventually, we were able to cover at each telescope pointing approximately 3 times more area than the basic NICMOS/3 field of view.

For our scanning pattern we took advantage of the relative alignment of ACS and WFPC2 on the HST focal plane. As shown in Figure 1, a diagonal shift of WFPC2 along the chevron direction corresponds almost exactly to exchanging the two CCD detectors of ACS. The strips were typically 12 pointings long, and adjacent strips were carefully matched to provide full WFPC2 coverage of the field with modest overlap. One strip every three was taken with the telescope rotated by 180 degrees, in order to virtually exchange ACS and WFPC2 and ensure maximum overlap between the two instruments. The two HST orientations were 100° (35 orbits, Fall 2004) and 280° (69 orbits, Spring 2005).

The overall field covered by the program is shown in Figure 2, over plotted on the 2MASS K-band image of the Orion Nebula. The area imaged with ACS and WFPC2 is approximately 1/6 of a square degree, whereas the NICMOS data cover approximately 120 square arcmin.

3. Data products

We cannot give here a full account of the data reduction steps required to produce science quality images and photometry from our dataset. The standard HST pipeline had to be complemented by a number of special tools in order to deal with the effects arising from the unusual extension and brightness of the target and from our observing strategy. For example, we had to face the issue of the positioning all tiles on an absolute

https://doi.org/10.1017/S1743921305004746 Published online by Cambridge University Press

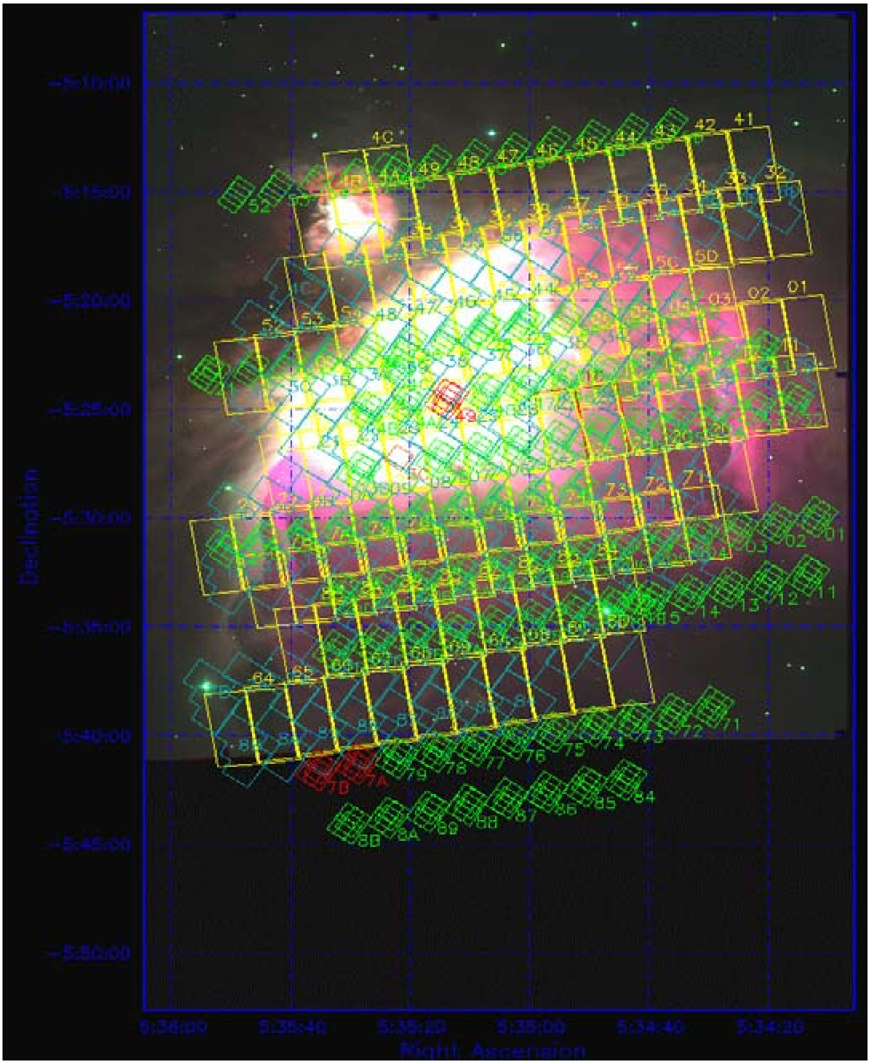

Figure 2. The area covered by the survey. The colors label different instruments: ACS (yellow), WFPC2 (cyan) and NICMOS (green). The red areas represent missed or repeated observations. For the orginal colour figure, see the electronic version of this proceedings (http://journals.cambridge.org/jid_IAU).

astrometric reference, the handling of time-variable objects in the overlapping drizzled data, fringing in the F850LP filter varying with position inside the nebula, photometry of saturated stars (possible with the gain setting we used for ACS), the effect of blooming in the drizzled data, vignetting at the edge of NICMOS field probed by the FOM offsets, etc.

Photometry was obtained using both aperture and, when possible, PSF photometry, using daophot, SExtractor and HSTphot. All sources filters are individually examined for residual problems due e.g. to unproper cosmic rays removal (either missed or misidentified due to source variability), presence of close companions or circumstellar features, etc. We detected across the nebula a substantial number of galaxies in our red ACS filters and with NICMOS, and these also need to be identified and flagged.

https://doi.org/10.1017/S1743921305004746 Published online by Cambridge University Press

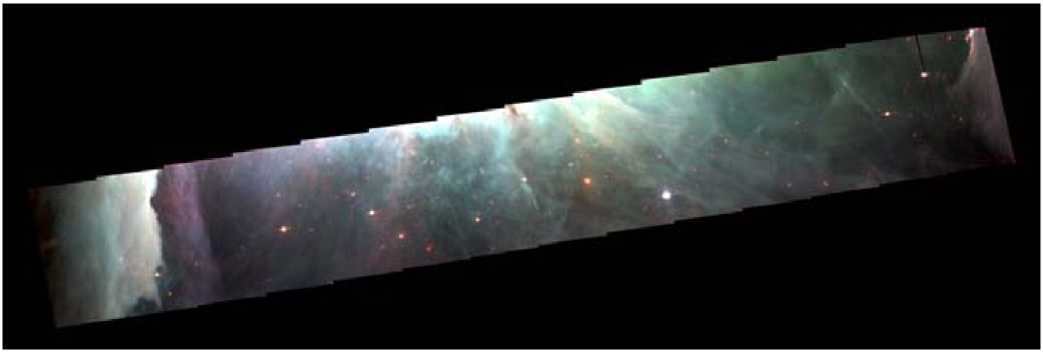

Figure 3. Color composite of an ACS strip observed in the Fall 2004 campaign.

The delivered data products will include, together with the final images on a common coordinate system, the main photometric catalog and an atlas of peculiar sources (binaries or multiple systems, disks and proplyds, galaxies, etc.).

4. A first look to an ACS strip

As an example, we present preliminary results obtained using aperture photometry on a strip taken with ACS in the Fall 2004 campaign. The strip (Figure 3) is a mosaic of 13 pointings in F435W, F685N and F850LP filters. At full resolution the original mosaic is an image of at least 30,000 by 10,000 pixels, hardly manageable with current standard astronomical packages. In Figure 4a) we present the color-magnitude diagram for the two reddest ACS filters, F775W and F850LP, obtained from single aperture photometry on a 2$\times$ rebinned version of the full strip. The plot uses different symbols and colors to represent the stars originally listed in the Hillenbrand (1997) catalog. With respect to the Hillenbrand sample the ACS data go approximately 5 mag deeper, down to F775W$\simeq$23 mag where our preliminary measures show errors of $\approx$0.25 mag. The F850LP photometry is entirely new.

In Figure 4a) the bright stars occupy a diagonal strip limited to the left by the 1 Myr isochrone (not shown in the figure). The width of the strip is most probably dominated by different values of the stellar extinction among otherwise similar stars. At $I \simeq 18$ mag we have PMS with mass corresponding to the H-burning limit. The strip appears to continue, albeit with significantly decreased density, at fainter luminosity levels characteristic of young substellar objects. Overall, however, the sample becomes richer of relatively blue objects, typically background sources. In Figure 4b) we show the star counts for the F775W filter, together with the histogram relative to the Hillenbrand (1997) sources. The distribution clearly shows a characteristic bimodal distribution, with a first peak at $I \sim 13$–17 mag corresponding to PMS stellar objects of the cluster and a second peak due to background objects. The NICMOS data fully confirm this behavior, which has also been recently evidenced in the deep Gemini near-IR photometry by Lucas, Roche & Tamura 2005.

The relative distribution of bright vs. faint sources clearly reveals strong variations in the background absorption of OMC-1. In Figure 5 we plot the positions of all sources detected in the F775W strip (top) and then only of the faint ones (middle) and of bright ones (bottom). While the bright sources appear uniformly distributed across the field, as expected for cluster members, the faint sources appear clustered at least in a couple of positions, corresponding to holes through the OMC-1 background. The presence of holes

https://doi.org/10.1017/S1743921305004746 Published online by Cambridge University Press

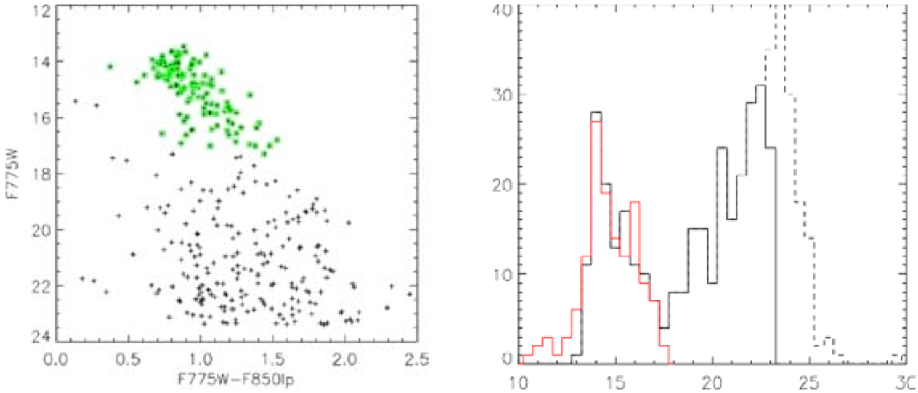

Figure 4. a, left) color-magnitude diagram for the F775W and F850LP ACS filters. The green squares label the sources present in the Hillenbrand (1997) catalog; b, right) stellar counts for the F775W filter. The red histogram represent the values reported by Hillenbrand (1997), whereas the dashed lines limits the locus of the faint stars with photometric accuracy worse than ≃0.3 mag.

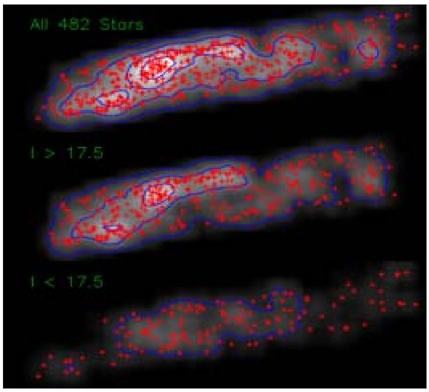

Figure 5. Position (crosses) and isodensity contours (blue solid lines) of the F775W sources identified in the strip presented in Figure 3. From top to bottom: all sources, faint sources ($m > 15.5$) and bright sources ($m < 18.5$).

through the nebula opens the possibility of obtaining the annual parallax of the OMC, using the exquisite sensitivity and spatial resolution of ACS to measure the systematic displacement of the bright stars vs. the faint ones. An HST proposal in this direction has been approved for the current Cycle 14 period.

References

Herbst, W., Bailer-Jones, C. A. L., Mundt, R., Meisenheimer, K. & Wackermann, R.2002 *A&A* 396, 513

Hillenbrand, Lynne A. 1997, *AJ* 113, 1733

Hillenbrand, Lynne A. & Carpenter, John M. 2000, *ApJ* 540, 236

Lucas, P. W. & Roche, P. F 2000, *MNRAS* 314, 858

Lucas, P.W., Roche, P.F. & M.Tamura, M. 2005 *mnras* in press

Luhman, K. L., Rieke, G. H., Young, Erick T., Cotera, Angela S., Chen, H., Rieke, Marcia J., Schneider, Glenn & Thompson, Rodger I. 2000, *ApJ* 540, 1016

Muench, August A., Lada, Elizabeth A., Lada, Charles J. & Alves, João 2002, *ApJ* 573, 366

https://doi.org/10.1017/S1743921305004746 Published online by Cambridge University Press